Full color natural light holographic camera

Myung K. Kim

Digital Holography and Microscopy Laboratory, Department of Physics, University of South Florida, Tampa, FL 33620, USA
mkkim@usf.edu

Abstract: Full-color, three-dimensional images of objects under incoherent illumination are obtained by a digital holography technique. Based on self-interference of two beam-split copies of the object's optical field with differential curvatures, the apparatus consists of a beam-splitter, a few mirrors and lenses, a piezo-actuator, and a color camera. No lasers or other special illuminations are used for recording or reconstruction. Color holographic images of daylight-illuminated outdoor scenes and a halogen lamp-illuminated toy figure are obtained. From a recorded hologram, images can be calculated, or numerically focused, at any distances for viewing.

OCIS codes: (090.1705) Color holography; (090.1995) Digital holography; (110.6880) Three-dimensional image acquisition.

References and Links

1. P. Hariharan, *Optical Holography: Principles, Techniques, and Applications* (Cambridge University, 1996).
2. D. Gabor, "A new microscopic principle," Nature **161**(4098), 777–778 (1948).
3. D. Gabor, "Microscopy by reconstructed wavefronts," Proc. Roy. Soc. **A197**, 454–487 (1949).
4. E. N. Leith and J. Upatnieks, "Wavefront reconstruction with continuous-tone objects," J. Opt. Soc. Am. **53**(12), 1377–1381 (1963).
5. E. N. Leith and J. Upatnieks, "Wavefront reconstruction with diffused illumination and three-dimensional objects," J. Opt. Soc. Am. **54**(11), 1295–1301 (1964).
6. S. A. Benton, "Hologram reconstructions with extended incoherent sources," J. Opt. Soc. Am. **59**, 1545 (1969).
7. S. A. Benton, "Holographic displays - a review," Opt. Eng. **14**, 402–407 (1975).
8. H. M. A. El-Sum and P. Kirkpatrick, "Microscopy by reconstructed wavefronts," Phys. Rev. **85**, 763 (1952).
9. E. N. Leith and J. Upatniek, "Holography with achromatic-fringe systems," J. Opt. Soc. Am. **57**(8), 975 (1967).
10. F. Dubois, L. Joannes, and J. C. Legros, "Improved three-dimensional imaging with a digital holography microscope with a source of partial spatial coherence," Appl. Opt. **38**(34), 7085–7094 (1999).
11. G. Cochran, "New method of making fresnel transforms with incoherent light," J. Opt. Soc. Am. **56**(11), 1513 (1966).
12. S. G. Kim, B. Lee, and E. S. Kim, "Removal of bias and the conjugate image in incoherent on-axis triangular holography and real-time reconstruction of the complex hologram," Appl. Opt. **36**(20), 4784–4791 (1997).
13. G. Sirat and D. Psaltis, "Conoscopic Holography," Opt. Lett. **10**(1), 4–6 (1985).
14. L. M. Mugnier and G. Y. Sirat, "On-axis conoscopic holography without a conjugate image," Opt. Lett. **17**(4), 294–296 (1992).
15. T.-C. Poon, M. H. Wu, K. Shinoda, and T. Suzuki, "Optical scanning holography," Proc. IEEE **84**(5), 753–764 (1996).
16. T. C. Poon, "Optical scanning holography - A review of recent progress," J. Opt. Soc. Korea **13**(4), 406–415 (2009).
17. G. Popescu, T. Ikeda, R. R. Dasari, and M. S. Feld, "Diffraction phase microscopy for quantifying cell structure and dynamics," Opt. Lett. **31**(6), 775–777 (2006).
18. C. Iemmi, A. Moreno, and J. Campos, "Digital holography with a point diffraction interferometer," Opt. Express **13**(6), 1885–1891 (2005).
19. V. Micó, J. García, Z. Zalevsky, and B. Javidi, "Phase-shifting Gabor holography," Opt. Lett. **34**(10), 1492–1494 (2009).
20. J. Rosen and G. Brooker, "Digital spatially incoherent Fresnel holography," Opt. Lett. **32**(8), 912–914 (2007).
21. J. Rosen and G. Brooker, "Fluorescence incoherent color holography," Opt. Express **15**(5), 2244–2250 (2007).
22. J. Rosen and G. Brooker, "Non-scanning motionless fluorescence three-dimensional holographic microscopy," Nat. Photonics **2**(3), 190–195 (2008).
23. M. K. Kim, "Adaptive optics by incoherent digital holography," Opt. Lett. **37**(13), 2694–2696 (2012).
24. M. K. Kim, "Incoherent digital holographic adaptive optics," Appl. Opt. **52**(1), A117–A130 (2013).

#185997 - $15.00 USD Received 26 Feb 2013; revised 2 Apr 2013; accepted 3 Apr 2013; published 11 Apr 2013

25. I. Yamaguchi and T. Zhang, "Phase-shifting digital holography," Opt. Lett. **22**(16), 1268–1270 (1997).
26. J. Kato, I. Yamaguchi, and T. Matsumura, "Multicolor digital holography with an achromatic phase shifter," Opt. Lett. **27**(16), 1403–1405 (2002).
27. J. Rosen, N. Siegel, and G. Brooker, "Theoretical and experimental demonstration of resolution beyond the Rayleigh limit by FINCH fluorescence microscopic imaging," Opt. Express **19**(27), 26249–26268 (2011).
28. M. Levoy, "Light fields and computational imaging," Computer **39**(8), 46–55 (2006).

1. Introduction

Photography records two-dimensional projection of the intensity profile of an object onto a fixed plane. In contrast, holography records sufficient information to be able to recreate the three-dimensional optical field emanating from an object, including both the amplitude and phase of the optical field [1]. The three-dimensional recording is made possible by the interference of the object's optical field and the reference optical field, and therefore requires coherence between the two. In D. Gabor's original conception, the reference is realized from a part of the illumination undisturbed by the object [2, 3]. The invention of the lasers made it possible, first by Leith and Upatnieks, to provide coherent reference field explicitly, and with high degree of freedom in the optical configurations [4, 5]. The three-dimensional holographic images quickly captured imagination of the general public, as well as leading to a multitude of new technological applications. The coherence is thus at the core of the holographic principle, but it has also been a major impediment to a wider range of applications of holography, requiring special illumination sources such as lasers or significantly constraining the optical configurations. While practical methods have been successfully developed for *displaying* holograms using incoherent illumination, such as rainbow holograms and white light holograms [6–8], *recording* of holograms under incoherent illumination has been more problematic, until recently.

A number of principles have been proposed since early in the development of conventional, i.e. analog, holography to record holograms using incoherent sources [9]. Note that low coherence sources can be used in interference microscopy or digital holography for phase microscopy of thin objects [10]: the object field is coherent within the coherence length. A different approach is needed for objects with spatial incoherence, such as generating two copies of the object field and arranging for self-interference between them. Examples include triangular interferometer [11, 12] and conoscopic holography [13, 14]. But in analog holography, such holograms of objects consisting of more than a few point sources are completely impractical because of the rapid accumulation of incoherent background. As described below, digital holography implementation of self-interference turns out to be a key to realizing holography of incoherent object fields.

Feasibility of digital holography for incoherent sources was first demonstrated by T.-C. Poon in a clever arrangement of projecting and scanning a Fresnel zone pattern over an object, together with electronic deconvolution of point detector signal [15, 16]. Holographic, i.e. three-dimensional, imaging of fluorescence has been demonstrated, but the complexity and low speed of the scanning system make practical applications difficult. A more fruitful approach has been the interference of the object field beam-split into two parts, and generation of the reference field by spatial filtering of one of the two components. Common-path or nearly common-path configurations make for high optomechanical stability, and high quality quantitative phase microscopy (QPM) images have been obtained [17–19]. But the spatial filtering limits the light efficiency and the method applies mostly to phase microscopy of thin objects. Instead of spatial filtering, introduction of differential curvature between the two copies encodes the three-dimensional positions of object points as Fresnel zone patterns of different frequencies and centers. For example, digital implementation of conoscopic and triangular holography have been demonstrated [12, 14], but the recent introduction of Fresnel incoherent correlation holography (FINCH) by J. Rosen fully demonstrated the ability to generate holographic images of incoherent object fields, including arc lamp illumination of macroscopic objects and 3D fluorescence microscopy [20–22].

#185997 - $15.00 USD Received 26 Feb 2013; revised 2 Apr 2013; accepted 3 Apr 2013; published 11 Apr 2013

This report is a demonstration of full-color holographic recording of outdoor scenes under natural daylight illumination, dubbed full-color self-interference incoherent digital holography (CSIDH). I have recently proposed and demonstrated highly effective means of aberration compensation in digital holography of incoherent optical field [23, 24]. The optical system is based on self-interference with differential curvature. Conceptually similar to FINCH, but in place of the spatial light modulator, a beam splitting prism and two mirrors of different curvatures are used to generate two copies of the object field. Superposition of the two copies with different curvatures leads to Fresnel zone pattern interference from each source point. The spatial incoherence of the object points leads to rapid build-up of incoherent background, which is removed by dithering one of the two mirrors in the interferometer, as in standard phase-shifting digital holography [25]. Detailed theoretical description of image formation by incoherent digital holography has been given in [24]. Several such phase shifted interference patterns are acquired by a color digital camera. The three RGB color channels are extracted and analyzed separately, generating a complex hologram by arithmetically combining the several frames of each channel. The resultant color hologram consists of three two-dimensional arrays of complex numbers, from which one can then numerically propagate to any distance to reconstruct the object's optical field. The three color channels are then recombined to generate the full color image of the object at the distance.

2. Experiment

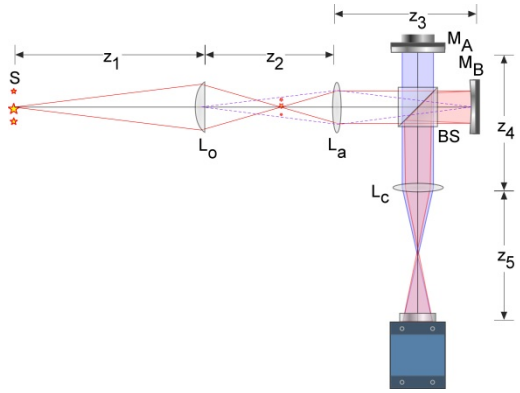

Fig. 1. Apparatus for CSIDH. L's: lenses; M's: mirrors; BS: beam-splitter.

The optical apparatus, Fig. 1, consists of the input optics, the interferometer, and the imaging optics. The input optics is a pair of lenses, with 25 cm and 10 cm focal lengths, to form a telescope. The interferometer consists of a beam-splitting cube and two mirrors. One is a plane mirror mounted on a piezo-actuator, which is driven by a function generator for phase shifting. The other is a curved mirror, of 60 cm focal length, to generate differential curvature. For imaging optics, a 10 cm lens is placed in front of the camera, for flexibility in magnification and physical dimensions of the apparatus. Approximately, the relevant distances are $z_2 \approx 35$ cm, and $z_3 \approx z_4 \approx z_5 \approx 20$ cm. A color CCD camera, Thorlabs CDU223C, with 1024 x 768 pixels, 4.76 x 3.57 mm sensor area and 8-bit pixel depth, is used for hologram capture. The three color channels have sensitivity peaks near 620 nm, 540 nm, and 460 nm for the red, green, and blue channels, respectively. The optical breadboard is mounted on a sturdy cart for portability.

#185997 - $15.00 USD Received 26 Feb 2013; revised 2 Apr 2013; accepted 3 Apr 2013; published 11 Apr 2013

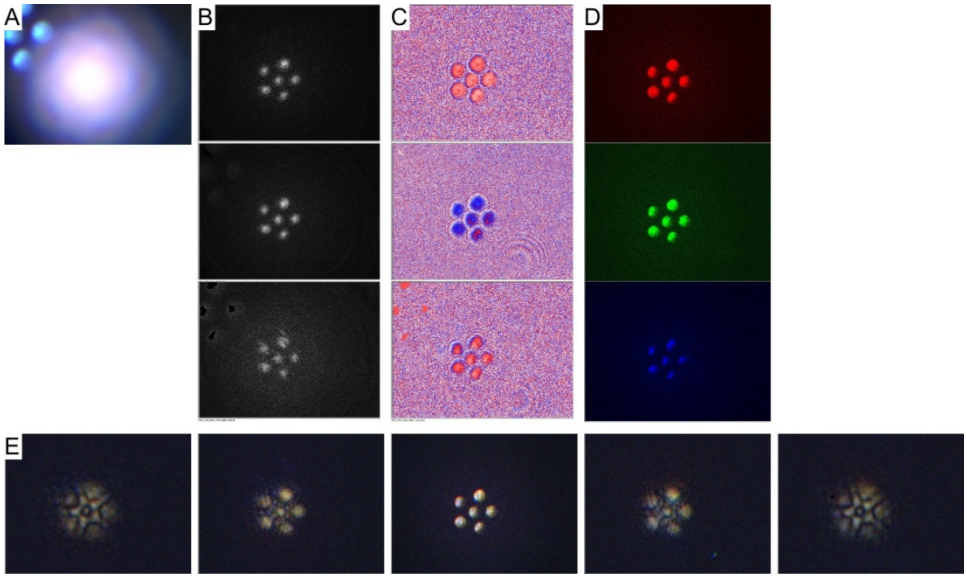

Fig. 2. CSIDH of a white LED flash light. (A) A frame capture of the CCD camera. (B) Amplitude and (C) phase of the complex hologram for the red, green, and blue channels. The phase images are plotted with blue-white-red color scale representing the range $[-\pi,\ \pi]$. (D) Numerically focused images from the hologram for the three color channels. (E) Full color holographic images. The best focus image in the middle panel is at 30 mm and the other panels are at 20 and 40 mm before and after the best focus.

Procedures for acquiring and reconstructing holographic images is described with the example of a white LED flashlight, Fig. 2. In order to obtain interference, first the distances of the two mirrors M_A and M_B are matched, usually using a single LED for better visibility. Panel (A) of Fig. 2 shows a frame captured by the CCD when we use a flash light containing six white LEDs. When the phase-shifting piezo-mount is dithering, one can discern the existence of interference in the center area of the large circular haze, but with just six LEDs, the background is already large and the fringe visibility quite low. The bright spots on the upper left is a stray reflection from the beam-splitter. It does not contribute to the interference or to the final holographic images. A ramp voltage is applied to the piezo-mount (150 nm/V nominal) with sufficient amplitude to cover more than 2π of phase shift. The camera frame rate or the piezo-ramp rate is adjusted so that N exposures are made over a 2π excursion. The complex hologram is calculated from the N intensity exposures I_n by $H=\sum_{n=0}^{N-1} I_n \exp\left(2\pi i n/N\right)/N$. Difficulties in phase-shifting for tri-color holography are the difference in the wavelengths of the three color channels and, therefore, in the necessary piezo-shifts [26]. Noting from the manufacturer data sheet that the wavelength peaks of the CCD sensitivity has close to $620:540:460 \approx 8:7:6$ ratio, the system is calibrated so that eight frames from a series of I_n is used to calculate the H_R for the red channel, while seven and six frames, respectively, are used for the green and blue channels. The complex holograms thus acquired are represented in Fig. 2(b) amplitude and Fig. 2(c) phase, for the three channels. These represent the starting optical field at the hologram plane, i.e. the camera plane. Numerical propagation to the image plane results in the image of the object for each channel (Fig. 2(d)), which can be then combined to form the full-color image, shown in the center panel of (Fig. 2(e)). The image distance is given by a combination of the z distances

#185997 - $15.00 USD Received 26 Feb 2013; revised 2 Apr 2013; accepted 3 Apr 2013; published 11 Apr 2013

and the focal lengths of Fig. 1 [24]. Numerical propagation to a range of distances around the focal distance demonstrates the focusing property of the holographic image (Fig. 2(e)).

3. Results

A few more examples are presented. In Fig. 3, the object is a toy boat, about 5 cm tall and placed about 1 m from the front lens of the apparatus, under illumination of a miniature halogen lamp. A die is also present in front of the boat. The complex hologram, acquired as described above, is shown in Fig. 3(a) for the red channel. The numerically focused images for the three color channels in Fig. 3(b) are combined to form the RGB color image (Fig. 3(d)). Much of the details of the boat, including the masts and the net, are reproduced. Focusing on different parts of the structure has been observed when reconstruction distance is varied. For comparison, a cell phone camera picture of the toy boat is shown in Fig. 3(c). The red content of the halogen lamp gives the image an overall orange-red tint. As a rudimentary means of color balance, each color frame is multiplied by a factor to equalize the frame averages of the three channels. Also, as an automatic brightness control, all three channels are multiplied by a factor to maintain the overall brightness to a desired level. These are only for the purpose of adequate rendering of the final images. In Fig. 3(e), the holographic image is focused to five distances –40, –20, 0, + 20, + 40 mm from the best focal distance 30 mm in the hologram space. The center frame of Fig. 3(e) is a copy of Fig. 3(d).

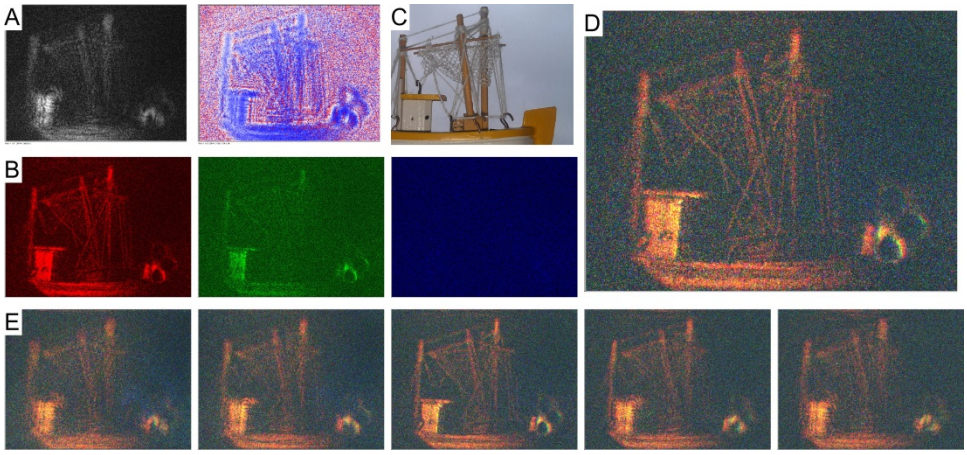

Fig. 3. CSIDH of a toy boat and a die under halogen lamp illumination. (A) Amplitude and phase of the hologram for the red channel. (B) Numerically focused images from the hologram for the three color channels. (C) A cell phone camera image for comparison. (D) Full color focused image. (E) Full color image at distances 20 and 40 mm before and after the best focus, at 30 mm.

A similar set of figures are given in Fig. 4, where the holographic camera is now turned toward a scene outside my office window, in clear daylight, looking at an apartment building with red roof and a garage building of USF physical plant. In Fig. 4(d), the red roof building is slightly out of focus, while the storage building with garage doors is in better focus. These structures are estimated to be at distances of about 1.0 and 0.5 km, respectively, and the field of view is about three degrees.

To demonstrate the three-dimensional content of the holographic images, Fig. 5 shows another example of the daylight outdoor scene plus the toy boat placed in front of the window and illuminated with a halogen lamp. A video clip is produced from a series of 100 frames of holographic images calculated at distances from 0 to 100 mm at 1 mm interval, starting from a single tri-color complex hologram. Two frames of the move show in Fig. 5(a) the boat clearly in focus, at about 30 mm, and the distant buildings out of focus, while conversely in Fig. 5(b) the storage building clearly in focus, at about 60 mm, and the boat out of focus.

#185997 - $15.00 USD Received 26 Feb 2013; revised 2 Apr 2013; accepted 3 Apr 2013; published 11 Apr 2013

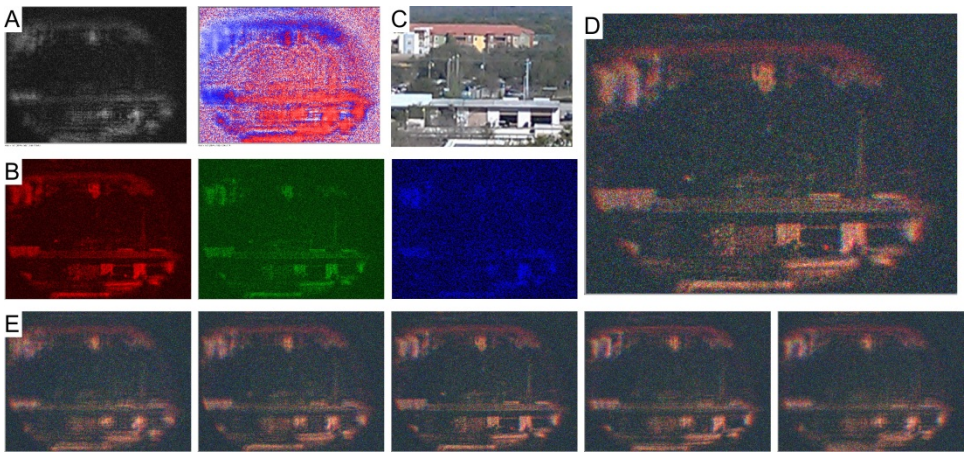

Fig. 4. CSIDH of an outdoor scene under clear daylight illumination. (A) Amplitude and phase of the hologram for the red channel. (B) Numerically focused images from the hologram for the three color channels. (C) A cell phone camera image for comparison. (D) Full color focused image. (E) Full color image at distances 20 and 40 mm before and after the best focus, at 60 mm.

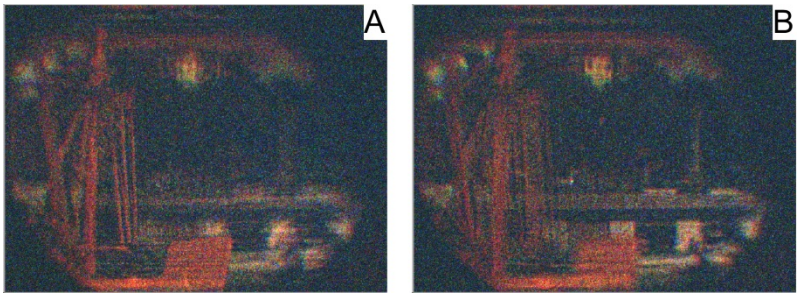

Fig. 5. (Media 1) A movie demonstrating the focusing property of a CSIDH. Frames of the movie are calculated at distances 0 ~100 mm, at 1 mm interval, from the same recorded hologram. Two frames from the movie show the image focused (A) on the close toy boat, at about 30 mm, and (B) on the distant buildings, at about 60 mm.

4. Discussion and conclusions

The examples clearly demonstrate the feasibility of full color natural light holographic 3D imaging. As proof-of-principle examples, the images are not yet perfect and some of the technical issues can be mentioned. To avoid vignetting and to image larger field of view, the interferometer needs to be configured more compactly, which should also improve the signal strength. The signal strength, however, may more directly increase with the bit depth of the CCD pixels – e.g., 12 bits instead of 8 bits – in order to extract weak interference fringes against large background. The lens and mirror systems are not presently optimized for best resolution [27]. As with most color cameras, the color rendering is imperfect and subject to somewhat arbitrary adjustments, but the examples do clearly demonstrate the ability to distinguish different colors with plausible consistency. A more important issue for improving the chromatic and overall performance is in the phase-shifting. At present the phase shifts are only approximate and rather inefficient for the three color channels. Still the overall performance of this early prototype appears quite robust against some of these deficiencies.

Using a simple optical apparatus, consisting of a beam splitter, a piezo-mounted plane mirror, a curved mirror, and a few lenses, together with a color camera and straightforward algorithms, three-dimensional holographic images are recorded and reconstructed under natural light illumination and with full color rendition. The simplicity of the principle

#185997 - $15.00 USD Received 26 Feb 2013; revised 2 Apr 2013; accepted 3 Apr 2013; published 11 Apr 2013

suggests possible extensions in non-optical regions of the electromagnetic spectrum, such as in THz, x-ray, as well as electron holography, where the beam-splitter-plus-two-mirror interferometer may be replaced with half-transparent Fresnel zone plates for these wavelengths, in more close analogy with the original FINCH interferometer. Three or more of the zone plates may be fabricated for phase-shift acquisition. More immediate and quite obvious suggestion is a consumer level holographic color camera, in basically a point-and-shoot configuration. In this respect, this holographic camera is to be compared with a system known as light-field camera, which is based on integral imaging principle using a lenslet array placed in front of the CCD sensor [28]. In comparison with such light-field camera, the holographic camera will have no loss of resolution due to the lenslets and the computational load will be substantially lighter. Incoherent light holographic cameras, such as proposed here, have real potential to make holographic 3D imaging as common as photography in all areas of imaging from microscopy to astronomy, as well as in engineering, artistic, and general public uses. More significantly, a large array of powerful holographic techniques developed for coherent imaging systems may now be applicable to incoherent imaging systems.

#185997 - $15.00 USD Received 26 Feb 2013; revised 2 Apr 2013; accepted 3 Apr 2013; published 11 Apr 2013